

Available online at www.sciencedirect.com

Procedia Engineering 14 (2011) 2459–2467

**Procedia
Engineering**

www.elsevier.com/locate/procedia

The Twelfth East Asia-Pacific Conference on Structural Engineering and Construction

Mathematical Simulation of Cross-Wind Vibrations in a Mono-Cable Chair Ropeway

R. Petrova^{1a}, St. Karapetkov¹, S. Dechkova^{1b} and Pl. Petrov²¹ Faculty of Engineering and Pedagogy, Technical University of Sofia, Bulgaria² Faculty of Mathematics and Informatics, University of Sofia, Bulgaria

Abstract

In recent years, chair ropeways used in skiing grounds or sightseeing places in Bulgaria have been adopted as basic means of transport, by virtue of their adaptability and low construction cost as compared to normal roads. However, the largest disadvantage of those cable structures is their weakness to wind influence. Because of their slender structure, transporters suspended by cables are easily affected by the drags of wind. The paper discusses the dynamic behaviour of the chairs and the rope in a span of a mono-cable chair ropeway. A 3D mechanical model of a multibody elastic system has been created. The chairs are presented as pendulums hanging on deformable elements whose elasticity depends on the position of pendulums inside the span and varies in time. The rope has been modelled as massless cable. Only the lateral vibrations of the rope, due to longitudinal motion of the chairs and gusts of the cross-wind loading have been studied. The wind is introduced as a uniform distributed load varying randomly in place and time. The dynamics of each chair has been described by differential equations whereas that of the rope has been expressed by partial differential equations. The slenderness of the supporting structure has been specially examined. All functions of the vertical and lateral vibrations and swinging of the chairs as well as the lateral macro-vibrations of the rope are numerical ones. The derived analytical equations are solved simultaneously by MatLab software. The results have been presented graphically and the simulation of the dynamic process has been animated. The created program is user-friendly and easily adaptable.

© 2011 Published by Elsevier Ltd. Open access under [CC BY-NC-ND license](https://creativecommons.org/licenses/by-nc-nd/4.0/).

Keywords: chair mono-cable ropeway, lateral wind, numerically solved dynamic equations

^a Corresponding author: Email: rpetrova123@abv.bg^b Presenter: Email: si_yana@abv.bg

1. INTRODUCTION

In recent years, chair ropeways used in skiing grounds or sightseeing places in Bulgaria have been adopted as basic means of transport, by virtue of their adaptability and low construction cost as compared to normal roads. However, the largest disadvantage of those cable structures is their weakness to wind influence. Because of their slender structure, transporters suspended by cables are easily affected by the drags of wind.

There are a lot of works studying the influence of the cross-wind on the ropeway, citing measurements (Hoffmann K. et al., 2004; Hoffmann K., 2004) or modeling the dynamics of the transport system (Kanki H. et al., 1994; Brownjohn J., 1998; Petrova et al., 2006). Some of the authors use finite-element method to solve the problems (Richter T., 1989; Petrova R., 2005), whereas others prefer to use other methods for numerical simulation (Engel E., 1994; Dragsits H., 2002).

2. MODEL OF THE ROPEWAY SYSTEM



Figure 1. Photo of the studied mono-cable chair ropeway

This is a small mono-cable ropeway with fixed double-seated chairs. It was built in the 70s of the last century near the town of Sliven, Bulgaria and is basically used for sightseeing because of the picturesque scenery. The ropeway covers a distance of about 1800m and an altitude of approximately 570m. There are 20 towers supporting the rope. The distance between the chairs depends on the number of the passengers. The ropeway operation upwards is simulated.

2.1. Spatial Model of a Chair

To obtain the equivalent mechanical model of a chair, a finite element model (FEM) has been developed. Constructive drawings have been used to create 3D models (fig.2), using software SolidWorks. Similar models have been already presented in (Petrova R. et al., 2009, Slavcheva J. et al., 2009). The authors use them for more precise calculation of mass and other inertia parameters of the equivalent pendulum.

The chair was modeled as a rigid pendulum, supported by the rope (fig.2d). The supporting point of the pendulum was marked with $A_i(x_i, y_i, z_i)$. It coincided with the clamp of the chair and moved along

the rope together with the rope itself. Its coordinates were calculated towards a moving coordinate system $O'_i y_i z_i$ along the undeformable inclined line of the rope. The pendulum had three degrees of freedom (DoF), corresponding to the following general coordinates: y_i - horizontal cross coordinate of point A_i ; z_i - vertical cross coordinate of point A_i and φ_i - angle of cross rotation of the chair. The entire mass was concentrated in the mass center of the chair, whose position varied, depending on the studied case (fig.2a,b,c). The value of the moment of inertia also depended on the studied case. Basically, the motion of the pendulum was spatial.

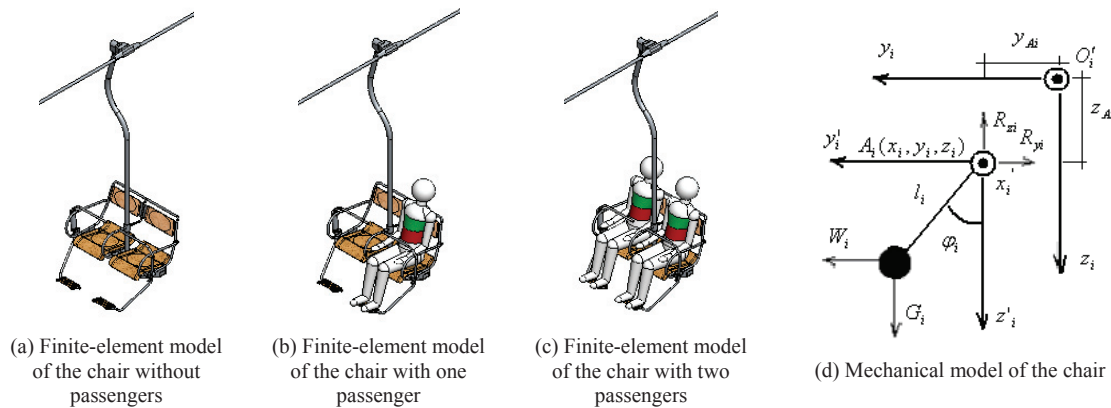


Figure 2: Models of the chair

The following assumption could be made: The rope moves constantly and all inertia forces in longitudinal direction equal to zero. Thus, in order to study the motion of the pendulum, we can study its motion along the rope as well as its relative motion in plane $O'_i y_i z_i$. The motion of the pendulum denoted i inside the span, is described by the following equations:

$$[A_i] \{\ddot{Q}_i\} = \{B_i\} \quad (1)$$

where $[A_i]$ is a symmetrical square matrix, whose elements introduce the coefficients in front of the derivatives of the general coordinates of pendulum; $\{\ddot{Q}_i\}$ is the array of the derivatives of all general coordinates of pendulum and $\{B_i\}$ is the array of all general loads applied to pendulum. Generally the matrix and the arrays equal to:

$$[A_i] = \begin{bmatrix} m_i & 0 & m_i l_i \cos \varphi_i \\ 0 & m_i & -m_i l_i \sin \varphi_i \\ m_i l_i \cos \varphi_i & -m_i l_i \sin \varphi_i & m_i l_i + J_i / l_i \end{bmatrix}; \quad \{\ddot{Q}_i\} = \begin{Bmatrix} \ddot{y}_i \\ \ddot{z}_i \\ \ddot{\varphi}_i \end{Bmatrix}; \quad (2a,b)$$

$$\{B_i\} = \begin{Bmatrix} m_i l_i \sin \varphi_i \cdot \dot{\varphi}_i^2 + W_i(x, t) - R_{yi}(x, t) \\ m_i l_i \cos \varphi_i \cdot \dot{\varphi}_i^2 + m_i g - R_{zi}(x, t) \\ W_i(x, t) l_i \cos \varphi_i - m_i g l_i \sin \varphi_i \end{Bmatrix} \quad (2c)$$

All symbols introduced in equations (1) and (2) are defined in table 1. All derivatives marked with dot introduce derivatives towards time like $\dot{x} = dx/dt$.

Table 1: Symbols, used to define the motion of the chair number i

Symbol	identification	dimension
m_i	mass of the chair, including the mass of the passengers	kg
l_i	distance between the projections of the mass center of the chair and the mass center of the rope in plane $A_i y i z i$	m
J_i	inertia mass moment of the chair towards axis x_i perpendicular to plane $A_i y i z i$	kg.m ²
y_i	horizontal cross coordinate of the chair, marked in fig. 2d as y_{Ai}	m
z_i	vertical coordinate of the chair, marked in fig. 2d as z_{Ai}	m
φ_i	angle of cross rotation of the chair, marked in fig. 2d as φ_i	rad
g	earth acceleration, equals to 9.81	m/s ²
w_i	horizontal cross-wind force, acting at the chair and the passengers	N
κ_{yi}	horizontal cross elastic force, supporting the chair	N
κ_{zi}	vertical cross elastic force, supporting the chair	N

2.2. Mathematical Model of the Rope

The rope is modelled as massless deformable cable. All derived equations are based on the linear theory of cables and theory of ropeways (Czitary E., 1962; Дивизиов В., 1975). All equations are true only for a fixed moment of time. As the rope is a massless body there are no inertia forces due to its motion.

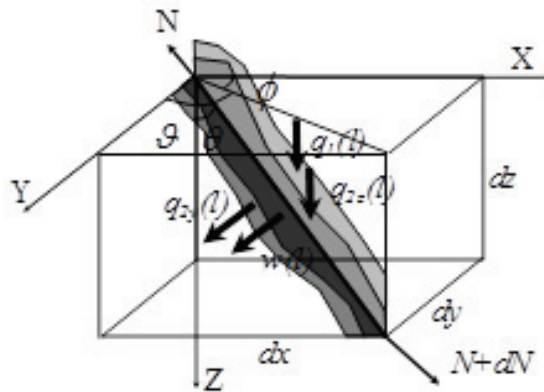


Figure 3. An elementary part of the rope

We examine the equilibrium of the elementary part of the rope with length of dl , shown in fig. 3. It is loaded by distributed loads, as follows: $q_1(l)$ - dead weight of the rope, [N/m]; $q_{2z}(l)$ - vertical loads from the chairs, [N/m]; $q_{2y}(l)$ - cross horizontal loads from the chairs, [N/m] and $w(l)$ - cross-wind loads, [N/m]. The tensile inner force in the rope is N . The angle between the rope and the vertical axis is θ , while the two horizontal angles, as shown in fig. 3, are marked with ϕ - towards X and ϑ - towards Y . The tensile force in the rope is T . We accept the longitudinal horizontal projections of T , marked with T_x are equal in the two outer sides of the part.

The equilibrium equations of the studied elementary part of the rope are:

$$\begin{aligned}
\sum X_i = 0 : & \quad N \sin \theta \cos \phi = (N + dN) \sin(\theta + d\theta) \cos(\phi + d\phi) = T_x \\
\sum Y_i = 0 : & \quad -N \sin \theta \sin \phi + (N + dN) \sin(\theta + d\theta) \sin(\phi + d\phi) + w(l)dl + q_{2y}(l)dl = 0 \\
\sum Z_i = 0 : & \quad -N \cos \theta + (N + dN) \cos(\theta + d\theta) + q_1(l)dl + q_{2z}(l)dl = 0
\end{aligned} \quad (3)$$

Considering that $dl^2 = dx^2 + dy^2 + dz^2$, we obtain the following equation $dl = dx \sqrt{1 + (y')^2 + (z')^2}$, where $y' = dy/dx$ and $z' = dz/dx$. All derivatives, marked with apostrophe are derivatives towards one of the axes. We assume also that angle of ϕ is a small angle, normally smaller than 1° , so we can write that $dl = dx/(\sin \theta \cos \phi) \approx dx/\sin \theta$ as $\cos \phi \approx 1$ (fig. 3). Assuming the above mentioned we transform the second equation in eq.3 as:

$$\left(\frac{w(l)}{\sin \theta} + \frac{q_{2y}(l)}{\sin \theta} \right) dx = -T_x \cdot d(\tan \phi) = -T_x \cdot d\left(\frac{dy}{dx} \right) = -T_x \cdot dy' \quad (4)$$

Similarly, assuming that $\cos(\phi + d\phi) \approx \cos \phi$, we can transform the last equation of eq.3 as:

$$\left(\frac{q_1(l)}{\sin \theta} + \frac{q_{2z}(l)}{\sin \theta} \right) \cos \phi \cdot dx = -T_x \cdot d(\cot \theta) = -T_x \cdot d\left(\frac{dz}{dx} \right) = -T_x \cdot dz' \quad (5)$$

Thus, the equilibrium of the rope can be described by the following partial differential equations:

$$\begin{cases}
y'' = -\frac{1}{T_x} \left(\frac{w(l)}{\sin \theta} + \frac{q_{2y}(l)}{\sin \theta} \right) \\
z'' = -\frac{1}{T_x} \left(\frac{q_1(l)}{\sin \theta} + \frac{q_{2z}(l)}{\sin \theta} \right)
\end{cases} \quad (6)$$

2.3. Mathematical model of the cable structure

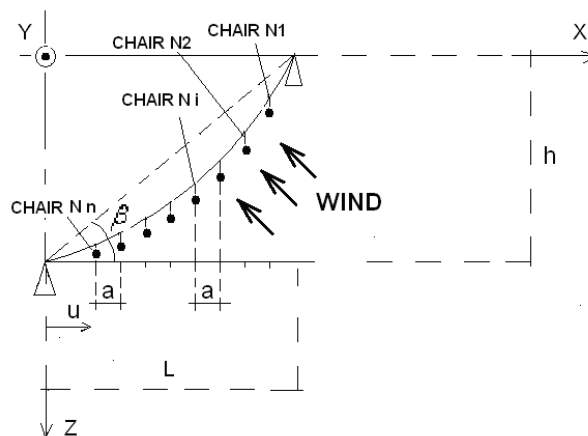


Figure 4. Scheme of the studied span

We examine only one span of the rope (fig. 4). The horizontal distance between the towers is marked by L and the altitude displacement by h . The distance between the chairs is one and the same. Neglecting the tensile deformations of the rope and regarding that its deflection is much smaller than the other geometric dimensions, we can assume that the horizontal distance between the chairs is constant, denoted by a . The distance between the left tower and the nearest chair is marked by u .

Regarding the dead weight of the rope as constant, we can rewrite the above equations $q_l(l) = \text{const} = q_l$ and $q_l/\cos\beta = q_l(l)/\sin\theta$, where β is the angle of the altitude displacement of the span, as shown in fig. 4 and replacing the other loads with functions of coordinate x : $\bar{w}(x) = w(l)/\sin\theta$; $\bar{q}_{2y}(x) = q_{2y}(l)/\sin\theta$; $\bar{q}_{2z}(x) = q_{2z}(l)/\sin\theta$. The final result is:

$$\begin{cases} y'' = -\frac{I}{T_x}(\bar{w}(x) + \bar{q}_{2y}(x)) \\ z'' = -\frac{I}{T_x}\left(\frac{q_l}{\cos\beta} + \bar{q}_{2z}(x)\right) \end{cases} \quad (7)$$

The solution of the above stated partial differential equations is:

$$\begin{aligned} y &= C_1 + C_2x - \frac{I}{T_H} \left[\int_0^x \bar{w}(\eta)(x-\eta)d\eta + \int_0^x \bar{q}_{2y}(\eta)(x-\eta)d\eta \right] = y_w(x,t) + y_{q_2}(x,t) \\ z &= C_3 + C_4x - \frac{I}{T_H} \left[\frac{q_l}{2\cos\beta}x^2 + \int_0^x \bar{q}_{2z}(\eta)(x-\eta)d\eta \right] = z_{q_1}(x) + z_{q_2}(x,t) \end{aligned} \quad (8)$$

where C_i , $i = 1 \div 4$ are constants, depending on the boundary conditions.

The function $y_w(x,t)$ describes the influence of the cross-wind on the rope. We introduce the left coordinate of the loaded section inside the span with L_1 and the right coordinate with L_2 . The cross-wind load is a uniform distributed load, whose value is w and varies in time. For a fixed moment of time the functions in eq. 8 are:

$$y_w(x,t) = \begin{cases} 0 \leq x \leq L_1 & w(t) \frac{(L_2 - L_1)(2L - L_1 - L_2)}{2LT_x \cos\beta} x \\ L_1 \leq x \leq L_2 & -w(t) \frac{(x - L_1)^2}{2T_x \cos\beta} + w(t) \frac{(L_2 - L_1)(2L - L_1 - L_2)}{2LT_x \cos\beta} x \\ L_2 \leq x \leq L & w(t) \frac{(L_2^2 - L_1^2)}{2LT_x \cos\beta} (L - x) \end{cases} \quad (9a)$$

$$z_{q_1}(x) = \left(\frac{q_l h}{2T_x \sin\beta} - \frac{h}{L} \right) x - \frac{q_l}{2T_x \cos\beta} x^2 + h \quad (9b)$$

The two other functions $y_{q_2}(x)$ and $z_{q_2}(x)$ count the forces, supporting the chairs, i.e. elastic forces R_{yi} and R_{zi} for chair denoted i . The number of chairs inside the span depends on the length of the span L , the distance between the chairs a , the distance between the left tower and the nearest gondola u . The bend in the rope y'_{q_2} due to concentrated force R_{yi} is:

$$y'_{q2i} = \lim(y'_{q2i}(x+\varepsilon) - y'_{q2i}(x-\varepsilon)) = -\frac{R_{yi}}{T_x} \quad \text{where } \varepsilon \rightarrow 0; \quad y'_{q2i} = -\int \frac{\bar{q}_{2y}(x)}{T_x} dx; \quad R_{yi} = \int_{x_i-\varepsilon}^{x_i+\varepsilon} \bar{q}_{2y}(x) dx \quad (10)$$

We suppose that the deformed line of the rope consists of $n+1$ inclined lines, where n equals the number of the chairs inside the span. The lines to the left and to the right of the chair denoted i are described by the functions $y_{i-l,i}^{R_y}(x)$ and $y_{i,i+l}^{R_y}(x)$, i.e:

$$\text{for } \begin{cases} x_{i-l} \leq x \leq x_i & y_{i-l,i}^{R_y}(x) = d_{i-l,i}x + b_{i-l,i} \\ x_i \leq x \leq x_{i+l} & y_{i,i+l}^{R_y}(x) = d_{i,i+l}x + b_{i,i+l} \end{cases} \quad (11)$$

where constants $(d_{0,l}, \dots, d_{i-l,i}, d_{i,i+l}, \dots, d_{n,L})$ and $(b_{0,l}, \dots, b_{i-l,i}, b_{i,i+l}, \dots, b_{n,L})$ satisfy the boundary conditions. They equal to:

$$\begin{aligned} d_{i,i+l} &= -\frac{u}{T_x L} (R_{y1} + R_{y2} + \dots + R_{yn}) - \frac{l}{T_x L} (R_{y2}a + \dots + R_{yi}(i-l)a + \dots + R_{yn}(n-l)a) + \frac{l}{T_x} (R_{yi} + R_{yi+l} + \dots + R_{yn}) \\ b_{i,i+l} &= \frac{R_{y1}}{T_x} u + \frac{R_{y2}}{T_x} (u+a) + \dots + \frac{R_{yi}}{T_x} (u+(i-l)a) \end{aligned} \quad (12)$$

The function of the deformed line of the rope due to vertical supporting reactions is calculated in a similar way. Below these two functions are introduced as:

$$\begin{aligned} y_{q2}(x,t) &= -\frac{ux}{T_x L} \sum_{k=l}^n R_{yk}(x,t) + \frac{u}{T_x} \sum_{k=l}^i R_{yk}(x,t) + \frac{x}{T_x} \sum_{k=i+l}^n R_{yk}(x,t) + \frac{a}{T_x} \sum_{k=l}^{i-l} kR_{yk+l}(x,t) - \frac{ax}{T_x L} \sum_{k=l}^{n-l} kR_{yk+l}(x,t) \\ z_{q2}(x,t) &= -\frac{ux}{T_x L} \sum_{k=l}^n R_{zk}(x,t) + \frac{u}{T_x} \sum_{k=l}^i R_{zk}(x,t) + \frac{x}{T_x} \sum_{k=i+l}^n R_{zk}(x,t) + \frac{a}{T_x} \sum_{k=l}^{i-l} kR_{zk+l}(x,t) - \frac{ax}{T_x L} \sum_{k=l}^{n-l} kR_{zk+l}(x,t) \end{aligned} \quad (13)$$

2.4. Simulation of the Operation of the Ropeway

In order to simulate the operation of the ropeway a numerical model using MatLab, toolbox Simulink has been created. The differential equations (1) and the functions (13) are solved simultaneously for each integration step of the calculating process.

3. NUMERICAL EXAMPLE

The cited numerical data is for a span of a length of 160m and an altitude displacement of 65m. There are 7 or 8 chairs inside the span. The distance between the chairs is $a = 20m$. The mass of the empty chair equals to 66kg, while the mass of a passenger is assumed to be 80kg. The diameter of the rope is 0.04m. The chairs move upwards with a constant velocity of 1.8m/s. When a chair leaves the upper right side of span a new one enters from the left. It is accepted that chairs denoted 5,6,14,15 are empty; there are two passengers in chairs denoted 2,3,7,8,9,11,12 and the rest of the chairs carry only one passenger (fig.4). The simulation starts when the chair denoted 8 is at the lower tower of the span and ends when it leaves the span. The velocity of the wind is a random function of time (fig.5) and acts in the sector between $L_1 = 20m$ and $L_2 = 50m$. Its values are results of some previously performed measurements.

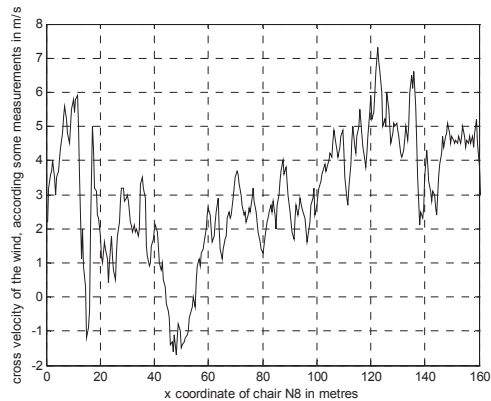


Figure 5. Cross velocity of the wind in the numerical example

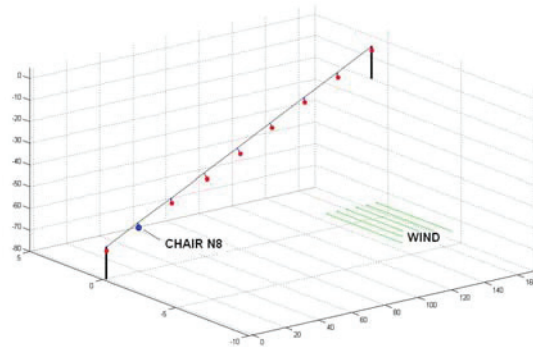
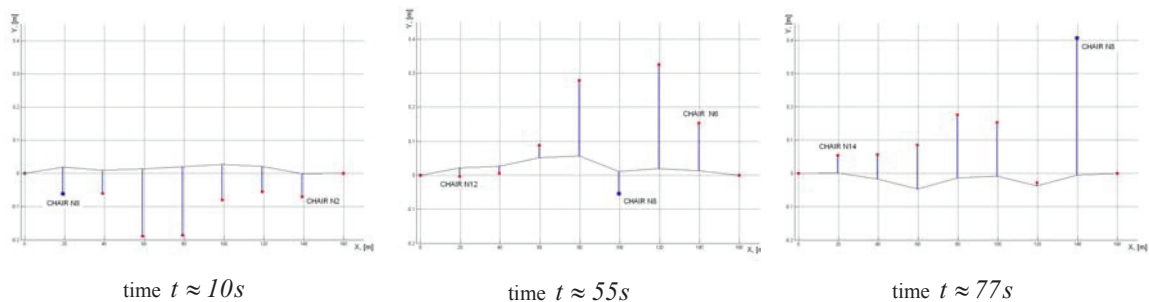


Figure 6. 3D animation of the working ropeway

Figure 7. Animation of the working ropeway seen from above (plane XY)

4. CONCLUSIONS

The presented work corresponds to the need of reconstruction of the modeled mono-cable chair ropeway. The created model enables the design engineers to study the interaction of the mass of the chair, the distance between the chairs, the tensile force in the rope and the dynamic phenomena in this slender structure. It allows performing numerical optimization of the operating ropeway aiming to reduce the lateral swinging and the other accompanying vibrations in order to increase the safety and comfort of the passengers. This model can easily be adapted for similar investigation of other mono-cable ropeways.

Acknowledgements

The present work has been carried out with the financial support of contract 102ПД091-16/2010, R&D sector of Technical University of Sofia, Bulgaria.

References

- [1] Brownjohn J. (1998). Dynamics of Aerial Cableway System, Engineering Structures, 20(9), pp 826-836
- [2] Czitary E. (1962), "Seilschwebebahnen", Wien, Springer-Verlag

- [3] Dragsits H. (2002). Untersuchung des Schwingungsverhaltens der Fahrbetriebsmittel einer Seilbahn - Anwendung genetischer Optimierungsverfahren, Diplomarbeit TU-Wien
- [4] Engel E., (1994). Ein diskretes Seilmodell, TU Wien, 21 Heft, pp.16-19
- [5] Hoffmann K. (2009), Oscillation Effects of Ropeways Caused by Cross-Wind and Other Influences, FME Transactions 37(4), pp. 175-184
- [6] Hoffmann K., Liehl R. (2004), Querschwingungen von ZUB- Fahrzeugen, Internationale Seilbahnrundschau, 8/2004
- [6] Kanki H., Y. Nekemoto, H. Monobe, H. Ogura, K. Kobayashi, (1994) Development of CMG Active Vibration Control Device for Gondola, JSME International Journal, Series C, 37(3)
- [7] Petrova R. (2005). Dynamic analysis of a chair ropeway, exposed to random wind loads, FME Transactions, 33(3), pp. 123-128
- [8] Petrova R., K. Hoffmann, R. Liehl (2006). Modelling and simulation of bicable ropeways under cross wind influence, Mathematical and Computer Modelling of Dynamical Systems, pp. 63-81
- [9] Petrova R., St. Karapetkov, S. Dechkova, J. Slavcheva (2009). Modal analysis of a chair of an aerial ropeway "Sliven – Karandila", accepted for publishing: Mechanics of Machines
- [10] Richter T. (1989). Schwingungsverhalten von einseil-umlaufbahnen beim anfahren und bremsen, D-r thesis, ETH – Zurich
- [11] Slavcheva J., R. Petrova, S. Dechkova (2009). Static analysis of a chair of an aerial ropeway "Sliven – Karandila", Mechanics of Machines, №84, pp. 45-48
- [12] Дивизиев В. (1975), "Възбуждени линии и кабелни кранове", Държавно издателство "Техника" София